

Inter-layer Hall effect in double quantum wells subject to in-plane magnetic fields

J. Kolorenč, L. Smrčka and P. Středa

*Institute of Physics, Academy of Sciences of the Czech Republic, Cukrovarnická 10, 162 53 Praha 6
(December 2, 2024)*

We report on a theoretical study of the transport properties of two coupled two-dimensional electron systems subject to in-plane magnetic fields. The charge redistribution in double wells induced by the Lorenz force in crossed electric and magnetic fields has been studied. We have found that the redistribution of the charge and the related inter-layer Hall effect originate in the chirality of diamagnetic currents and give a substantial contribution to the conductivity.

73.20.Dx, 73.40.Kp

I. INTRODUCTION

Semiconductor quantum wells, multi-wells and superlattices are designed to have an artificial electronic structure determined by their construction rather than by the properties of individual semiconductor materials¹. The band profiles of multi-wells are formed by a sequence of quantum wells separated by barriers. Electrons condense to two-dimensional (2D) electron layers localized in the wells and the tunnel-coupling of the layers leads to the formation of new electron systems, rich in optical and transport effects, that can be modified by application of the magnetic field.

Two experimental arrangements of the magnetotransport measurement in multi-well structures subjected to the in-plane magnetic field \vec{B} are possible: with the current \vec{j} flowing perpendicular to the magnetic field ($\vec{j} \perp \vec{B}$) or parallel with it ($\vec{j} \parallel \vec{B}$). The Hall effect plays a role in the case $\vec{j} \perp \vec{B}$. In wide *macroscopic* samples (superlattices) the standard method of the description of the Hall effect, via the inversion of the conductivity tensor, applies. This is no longer true for the double-well structures the width of which is *microscopic*. This is why we present here a novel theoretical approach to the calculation of the Hall effect, based on its textbook definition: the Hall electric field is caused by the accumulation of positive and negative charges on the opposite sample edges, induced by the Lorentz force.

The difference between conductivities along and perpendicular to the magnetic field direction was investigated experimentally in several papers,^{2–4}. The results, obtained by solving the Boltzmann equation⁵, have been found in a qualitative agreement with the experimental observation. However, no attention has been paid to the effect of the sample polarization due to the transfer of electrons between wells – to the Hall effect.

Let us consider the setup sketched in Fig. 1. The electrons are pushed by a Lorenz force from the left to the right well. Resulting non-equilibrium charge distribution gives rise to a potential that compensates for the Lorenz force in a similar way as the Hall voltage does in macroscopic samples. In a limiting case of very narrow wells,

the double-well system can be viewed as a parallel plate capacitor: the induced potential reduces to an inter-well Hall voltage U_H , a potential difference between electron systems in individual wells.

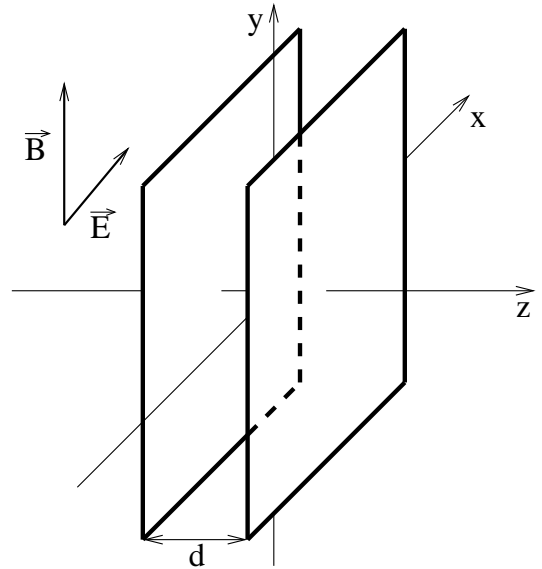


FIG. 1. Schematic picture of a double-layer system. Directions of applied electric and magnetic fields are indicated.

Note that in such an experimental arrangement the electron transport is closely related to the chirality of diamagnetic currents flowing in opposite directions in the left and right wells. In the thermodynamic equilibrium, the two currents are exactly balanced giving a zero net flow of electrons through the sample. In non-equilibrium states the electron system is polarized, more electrons are in the right well and an incomplete compensation of diamagnetic currents results in a finite transport current. The aim of this paper is to show that this usually neglected correction to the in-plane electrical conductivity gives a significant contribution for realistic double well structures.

For the sake of simplicity we employ the model of a double well described in a paper⁶. Two coupled, strictly two-dimensional electron layers confined in very narrow

potential wells are considered. Short-range scatterers, randomly distributed in individual wells, are assumed to be responsible for a finite relaxation time of electrons.

We use the *self-consistent* linear response theory (Kubo formula) in the random phase approximation (RPA) (see e.g. ⁸) to obtain the non-equilibrium charge distribution, the inter-layer Hall voltage and the conductivity tensor components.

II. MODEL HAMILTONIAN

In our model, the vector potential $\vec{A} = (zB, 0, 0)$ is used to describe the influence of the in-plane magnetic field $\vec{B} = (0, B, 0)$ on the electron structure of a double-layer system. The corresponding Hamiltonian reads

$$\hat{H}_0 = \frac{1}{2m^*} (\hat{p}_x + |e|Bz)^2 + \frac{1}{2m^*} (\hat{p}_y^2 + \hat{p}_z^2) + V(z), \quad (1)$$

where m^* denotes the electron effective mass and $V(z)$ is a confining potential with two deep minima at $z = \pm d/2$, $V(d/2) = V(-d/2)$. The subscript 0 denotes that no scattering mechanism is included. The form of (1) allows separation of variables, the x, y dependent part of eigenstates of \hat{H}_0 is the plain wave $|\vec{k}\rangle$ with the two-dimensional wave vector $\vec{k} = (k_x, k_y)$. To describe electron eigenstates depending on the remaining third coordinate z we restrict ourselves to the tight-binding approximation employing only the lowest eigenstates $|\varphi_\alpha(z)\rangle$ of uncoupled wells ^{5,6}. The index $\alpha = R, L$ distinguishes the right and left well. Thus, a complete single-layer eigenstate reads $|\varphi_\alpha, \vec{k}\rangle = |\varphi_\alpha(z)\rangle |\vec{k}\rangle$ and

$$\hat{P}_\alpha = \sum_{\vec{k}} |\varphi_\alpha, \vec{k}\rangle \langle \varphi_\alpha, \vec{k}| \quad (2)$$

has a meaning of a projection operator to the states in the well α , $\hat{P}_L + \hat{P}_R = 1$. The Hamiltonian (1) is diagonal in the index \vec{k} in our restricted basis and takes the matrix form

$$\langle \vec{k} | \hat{H}_0 | \vec{k}' \rangle = \delta_{\vec{k}, \vec{k}'} \begin{pmatrix} E_L(\vec{k}) & t \\ t & E_R(\vec{k}) \end{pmatrix}, \quad (3)$$

where $E_{L,R}(\vec{k})$ are single-well eigenenergies,

$$E_{L,R}(\vec{k}) = \frac{1}{2m^*} \left(\hbar k_x \mp \frac{1}{2} |e| B d \right)^2 + \frac{\hbar^2 k_y^2}{2m^*}. \quad (4)$$

The hopping integral t is given by $t = \langle \varphi_L | V(z) | \varphi_R \rangle = \langle \varphi_R | V(z) | \varphi_L \rangle$. Note that we neglected the effect of the in-plane field on the energy spectra of individual layers and that the z coordinate has been replaced in (4) by $\pm d/2$ for the right and left layer, respectively.

The diagonalization of the matrix (3) yields a pair of new eigenstates $|\chi_i^{(x)}(z)\rangle$. They depend only on the x component of \vec{k} and the index i equals b for the bonding

state and a for the antibonding state. The new basis $|\chi_i^{(x)}\rangle$ is related to the basis of single-well eigenstates $|\varphi_\alpha\rangle$ by

$$|\chi_{b,a}^{(x)}\rangle = \frac{1}{\sqrt{2}} \sqrt{1 \pm \Delta} |\varphi_L\rangle \pm \frac{1}{\sqrt{2}} \sqrt{1 \mp \Delta} |\varphi_R\rangle, \quad (5)$$

where $\Delta = \delta / \sqrt{\delta^2 + t^2}$ and δ is the abbreviation for $\hbar |e| d B k_x / 2m^*$. Then the eigenenergies of (1) reads

$$E_{b,a}(\vec{k}) = E_{b,a}^{(x)}(k_x) + \frac{\hbar^2 k_y^2}{2m^*}, \quad (6)$$

$$E_{b,a}^{(x)}(k_x) = \frac{\hbar^2 k_x^2}{2m^*} + \frac{e^2 d^2 B^2}{8m^*} \mp \sqrt{\delta^2 + t^2}.$$

The model is characterized by two parameters, the inter-layer distance d and the hopping integral t . It is a good approximation when the cyclotron energy and the tunnel coupling are small in comparison with the single-well quantization energies.

The Hamiltonian \hat{H} of the system with short-range scatterers is obtained by adding the impurity potential \hat{V}_{imp} to \hat{H}_0 . As mentioned above, we assume that impurities are distributed in both the left and right wells at random. To be more specific, the scattering on an individual impurity is considered to be intra-well (diagonal in the layer index α) and isotropic in \vec{k} direction. The finite lifetime and transport relaxation time result from replacing the quantities characteristic for a given configuration of scatterers by these quantities averaged over all possible configurations.

III. CHARGE REDISTRIBUTION

Let us first turn attention to the self-consistent procedure of establishing the non-equilibrium charge distribution and the Hall potential U_H in the RPA, as this is the novel feature of our approach to the theoretical description of magnetotransport in microscopically narrow systems.

The standard Kubo formula describing the linear response to a time-dependent perturbation operator \hat{H}_p is employed, our formalism is close to that used in ⁷. In our case, the operator \hat{H}_p is given as a sum of two parts: the externally applied potential represented by $\hat{H}_p^{(1)}$ and the self-consistent electric field of non-equilibrium electrons described by $\hat{H}_p^{(2)}$.

The external homogeneous electric field $\vec{\mathcal{E}} = (\mathcal{E}_x, \mathcal{E}_y)$ is included into the vector potential \vec{A} . Then the corresponding part of \hat{H}_p takes the form

$$\hat{H}_p^{(1)}(t) = \frac{e}{i\omega} \hat{\vec{v}} \cdot \vec{\mathcal{E}} e^{i\omega t}, \quad (7)$$

where $\hat{\vec{v}} = (\hat{v}_x, \hat{v}_y)$ is the velocity operator and ω denotes the frequency. This perturbation yields the static polarization of the sample and induces the stationary current in the limit $\omega \rightarrow 0$.

The second part of the perturbation Hamiltonian, denoted as $\hat{H}_p^{(2)}$, describes the Hartree potential derived from the non-equilibrium electron density by solving the Poisson equation. In our model, this potential reduces to the potential difference U_H between two 2D electron layers and the operator $\hat{H}_p^{(2)}$ can be written as

$$\hat{H}_p^{(2)} = e \frac{U_H}{d} \hat{z}, \quad \hat{z} = \frac{d}{2} (\hat{P}_R - \hat{P}_L). \quad (8)$$

Here \hat{z} stands for an operator of the z coordinate in the representation of single-layer eigenstates $|\varphi_\alpha\rangle$ and U_H has to be determined self-consistently.

We introduce δQ_α , the non-equilibrium charge density per unit area of a well α , as an expectation value of the operator

$$\hat{Q}_\alpha = e \hat{P}_\alpha = e \sum_{\vec{k}} |\varphi_\alpha, \vec{k}\rangle \langle \varphi_\alpha, \vec{k}|, \quad (9)$$

evaluated using the non-equilibrium density matrix. Due to the charge conservation δQ_R is equal to $-\delta Q_L$, and we can write δQ instead of δQ_R ($-\delta Q$ instead of δQ_L), for convenience.

In our model, the Hall potential calculated in the Hartree approximation, U_H , is related to the local non-equilibrium charge density δQ by a particularly simple formula

$$\delta Q = \varepsilon \frac{U_H}{d}. \quad (10)$$

This expression corresponds to the parallel plate capacitor in which the potential difference between plates is fully determined by their distance, the excess charge on one particular plate and the dielectric constant ε of the insulator between plates.

Since \hat{H}_p is a sum of $\hat{H}_p^{(1)}$ and $\hat{H}_p^{(2)}$, also the charge density δQ_α can be written as a sum of two contributions $\delta Q_\alpha^{(1)}$ and $\delta Q_\alpha^{(2)}$. Introducing the resolvents in the standard way by $\hat{G}^\pm(E) = (E - \hat{H}_0 - \hat{V}_{imp} \pm i0)^{-1}$ and $\delta(E - \hat{H}) = (i/2\pi)[\hat{G}^+(E) - \hat{G}^-(E)]$, we get the response to $\hat{H}_p^{(1)}$

$$\begin{aligned} \delta Q_\alpha^{(1)} &= i\hbar e^2 \mathcal{E}_x \int dE f_0(E) \\ &\times \text{Tr} \left\langle \delta(E - \hat{H}) \left[\hat{P}_\alpha \frac{d\hat{G}^+(E)}{dE} \hat{v}_x - \hat{v}_x \frac{d\hat{G}^+(E)}{dE} \hat{P}_\alpha \right] \right\rangle, \end{aligned} \quad (11)$$

in the limit $\omega \rightarrow 0$. Here $\langle \dots \rangle$ denotes the configuration averaging and f_0 stands for the Fermi-Dirac distribution function. As expected, the applied electric field \mathcal{E}_y does not induce any excess charge.

The response to the operator $\hat{H}_p^{(2)}$, defined by equation (8), yields

$$\begin{aligned} \delta Q_\alpha^{(2)} &= -\frac{e^2}{d} U_H \int dE f_0(E) \\ &\times \text{Tr} \left\langle \delta(E - \hat{H}) \left[\hat{z} \hat{G}^-(E) \hat{P}_\alpha + \hat{P}_\alpha \hat{G}^+(E) \hat{z} \right] \right\rangle. \end{aligned} \quad (12)$$

The equations (11) and (12) relate the induced charge densities to the applied electric fields \mathcal{E}_x and $\mathcal{E}_z = -U_H/d$ and their structure reminds the equation (10). Therefore, if we consider them as definitions of the generalized dielectric functions $\varepsilon^{(1)}$ and $\varepsilon^{(2)}$, we can write

$$\delta Q^{(1)} = \varepsilon^{(1)} \mathcal{E}_x, \quad \delta Q^{(2)} = \varepsilon^{(2)} \mathcal{E}_z, \quad (13)$$

where again the layer index is omitted and we have in mind the partial densities in the right well.

Making use of $\delta Q = \delta Q^{(1)} + \delta Q^{(2)}$, the decomposition of the local charge density δQ into two components, the self-consistent equation (10) takes the form

$$\varepsilon^{(1)} \mathcal{E}_x - \varepsilon^{(2)} \frac{U_H}{d} = \varepsilon \frac{U_H}{d}, \quad (14)$$

and its solution reads

$$\frac{U_H}{d} = \frac{\varepsilon^{(1)}}{\varepsilon^{(2)} + \varepsilon} \mathcal{E}_x. \quad (15)$$

This formula relates the self-consistent Hartree field of electrons to the x component of the externally applied electric field $\vec{\mathcal{E}}$, as we have anticipated in the introduction.

IV. IN-PLANE CONDUCTIVITY

With the established relations between U_H , δQ and \mathcal{E}_x , the calculation of the conductivity is a straightforward procedure. The components of the tensor $\vec{\sigma}$ are determined through the expectation values of the current operator

$$\hat{j} = e \hat{v} + \frac{e^2 \vec{\mathcal{E}}}{im^* \omega} e^{i\omega t}, \quad (16)$$

calculated using the non-equilibrium density matrix given by a response to the perturbation \hat{H}_p in the limit $\omega \rightarrow 0$.

Similarly as the generalized dielectric function ε , the conductivity tensor can be written as a sum of two contributions $\vec{\sigma}^{(1)}$ and $\vec{\sigma}^{(2)}$. The response to $\hat{H}_p^{(1)}$ leads to the standard expressions⁷ for the static conductivity $\vec{\sigma}^{(1)}$. We can write for its components

$$\begin{aligned} \sigma_{ss}^{(1)} &= \pi \hbar e^2 \int dE \left(-\frac{df_0(E)}{dE} \right) \\ &\times \text{Tr} \left\langle \delta(E - \hat{H}) \hat{v}_s \delta(E - \hat{H}) \hat{v}_s \right\rangle, \end{aligned} \quad (17)$$

where s stands for x or y . The form of expressions for $\sigma_{xx}^{(1)}$ and $\sigma_{yy}^{(1)}$ is the same, but an important difference stems from the fact that while $\hat{v}_y(-\vec{k}) = -\hat{v}_y(\vec{k})$, the breaking of the time reversal symmetry by $\vec{B} \perp x$ implies $\hat{v}_x(-\vec{k}) \neq -\hat{v}_x(\vec{k})$. Consequently, the evaluation of the

trace in (17) leads to substantially different results for $s = x$ and $s = y$.

The response to the self-consistent field described by the perturbation Hamiltonian $\hat{H}_p^{(2)}$ gives a non-zero value only for the current flowing along the x direction. The corresponding contribution to the conductivity reads

$$\sigma_{xx}^{(2)} = e^2 \frac{\varepsilon^{(1)}}{\varepsilon^{(2)} + \varepsilon} \int dE f_0(E) \times \text{Tr} \left\langle \delta(E - \hat{H}) \left[\hat{z} \hat{G}^-(E) \hat{v}_x + \hat{v}_x \hat{G}^+(E) \hat{z} \right] \right\rangle. \quad (18)$$

Thus, while the conductivity σ_{yy} is determined only by the external field \mathcal{E}_y and $\sigma_{yy} = \sigma_{yy}^{(1)}$, in the case of the x direction also the self-consistent Hall field U_H helps to conduct the current and $\sigma_{xx} = \sigma_{xx}^{(1)} + \sigma_{xx}^{(2)}$.

V. SHORT-RANGE SCATTERERS IN BORN APPROXIMATION

The primary aim of this paper is to estimate the importance of the contribution of $\sigma_{xx}^{(2)}$ to the conductivity σ_{xx} .

We have performed numerical calculation of these quantities for the realistic parameters of a bilayer system. The notably difficult problem is to model the electron scattering on impurities, as we have only limited knowledge about the nature of scatterers and their distribution in the sample. For simplicity, we assume the short-range scattering of electrons on impurities randomly distributed in both the left and right wells, as mentioned above. The concentration of impurities is assumed very low and the weak scattering on an individual impurity is treated in the Born approximation. The strength of the scattering on an individual impurity and the impurity concentrations are taken as adjustable parameters. Only the non-self-consistent version of the Born approximation is used which leads to inaccurate description close to singularities in the field dependence of $\vec{\sigma}$.

In the course of calculations, we apply the standard procedure of averaging the resolvents and their products over all possible configurations of impurities. We assume $\langle V_{imp} \rangle = 0$ as usual. The averaged resolvent $\langle \hat{G}^\pm(E) \rangle$ is approximated by $\overline{G}^\pm(E)$, which satisfies the coupled equations

$$\overline{G}^\pm(E) = \frac{1}{E - \hat{H}_0 - \hat{\Sigma}^\pm}, \quad (19)$$

$$\hat{\Sigma}^\pm = \langle \hat{V}_{imp} \overline{G}^\pm(E) \hat{V}_{imp} \rangle, \quad (20)$$

where $\hat{\Sigma}^\pm$ is the self-energy operator in the Born approximation, i.e. determined to the second order in the perturbation \hat{V}_{imp} .

The products $\langle \hat{G}^\pm \hat{v}_s \hat{G}^\pm \rangle$, $s = x, y$, appear in the expressions for conductivity. We approximate these expressions by the vertex functions $\hat{K}_s^{\pm\pm}$, which must be found by solving the Bethe-Salpeter equations. In the Born approximation, the equations take the form

$$\hat{K}_s^{\pm\pm} = \overline{G}^\pm \left(\hat{v}_s + \langle \hat{V}_{imp} \hat{K}_s^{\pm\pm} \hat{V}_{imp} \rangle \right) \overline{G}^\pm, \quad (21)$$

where $\langle \hat{V}_{imp} \hat{K}_s^{\pm\pm} \hat{V}_{imp} \rangle$ are the vertex corrections to the velocity component \hat{v}_s .

To proceed further, we accepted additional simplifications motivated by the very low scattering rate in high-mobility samples. Namely, the real part of the self-energy $\hat{\Sigma}^\pm$ (a correction to the eigenenergies) is neglected and only the terms of the lowest order of the scattering rate are kept in all expressions.

In this approximation, the imaginary part of the self-energy $\hat{\Sigma}^\pm$, denoted by $\hat{\Gamma}$, is diagonal in the spectral representation of the Hamiltonian H_0 and proportional to the densities of states, $g_\alpha = m^*/(\pi\hbar^2)$, of the uncoupled electron layers,

$$\Gamma_{b,a}(E, k_x) = \langle \chi_{b,a}^{(x)} | \hat{\Gamma}(E) | \chi_{b,a}^{(x)} \rangle = \pi\gamma_L(1 \pm \Delta)g_L + \pi\gamma_R(1 \mp \Delta)g_R. \quad (22)$$

The parameters γ_α represent the intra-well scattering rate and are given by the square of matrix elements of the single-impurity potential, multiplied by the concentrations of impurities. Thus, $\Gamma_{b,a}$ is determined as a weighted sum of scattering inside the left and right subsystems with the weights $1 \pm \Delta$.

It is also worth to know how the resulting quantities depend on the scattering rate. While $\sigma_{ss}^{(1)}$ and $\varepsilon^{(1)}$ would diverge in samples without impurities and the leading term of their power expansion is of the order $1/\Gamma$, $\sigma_{ss}^{(1)} \propto 1/\Gamma$ and $\varepsilon^{(1)} \propto 1/\Gamma$, the expressions obtained as the response to U_H will stay finite in this limit, $\varepsilon^{(2)} \propto 1$. Note that in spite of it $\sigma_{xx}^{(2)} \propto 1/\Gamma$ as $\sigma_{xx}^{(2)}$ is related to $\varepsilon^{(1)}$ through equation (18).

The vertex corrections vanish for the velocity component v_y and the product $\langle \hat{G}^\pm \hat{v}_y \hat{G}^\pm \rangle$ can be approximated by $\overline{G}^\pm \hat{v}_y \overline{G}^\pm$, as expected for randomly distributed short-range scatterers. This is not true for $\langle \hat{G}^\pm \hat{v}_x \hat{G}^\pm \rangle$. Due to the anisotropy of the scattering induced by the in-plane magnetic field, the vertex corrections have to be taken into account. We must solve two coupled Bethe-Salpeter equations for the vertex functions. Unfortunately, for our very simple model they are linearly dependent. Similar complication was found also in ⁵, where the same model was used to describe the electron transport by the Boltzmann equation. The second independent equation was supplied by the charge conservation rule $\delta Q_R = -\delta Q_L$.

VI. RESULTS AND DISCUSSION

The parameters corresponding to the sample B studied experimentally by Simmons et al.² are used in our model calculations. The distance between wells d equals 135 Å and the hopping integral t is supposed to be 0.9 meV. The density of electrons $N_e = 2.4 \times 10^{11} \text{ cm}^{-2}$ yields the Fermi energy 4.29 meV.

The applied in-plane magnetic field qualitatively changes the topology of Fermi contours^{2,5}. At zero field, the Fermi contours are two concentric circles. The larger circle corresponds to bonding states, the smaller one to antibonding states. The applied in-plane magnetic field shifts the centers of circles in the opposite directions in k space and gradually changes their shapes. The Fermi contour of the bonding subband acquires the shape of a “peanut”, the Fermi line of the antibonding subband evolves into a “lens” shape. The area of the lens is reduced by the increasing in-plane field. At the critical field $B_{c,1} = 7.4 \text{ T}$ the lens vanishes and the transition from two-component to one-component system occurs. The peanut splits at the higher critical field $B_{c,2} = 9.3 \text{ T}$ into two parts, the left and right electron layers become decoupled and two disconnected ovals represent the Fermi contours of individual layers above that field. The changes in the connectivity of Fermi lines are reflected in the field dependence of the density of electronic states (DOS) as van Hove singularities at the critical fields.

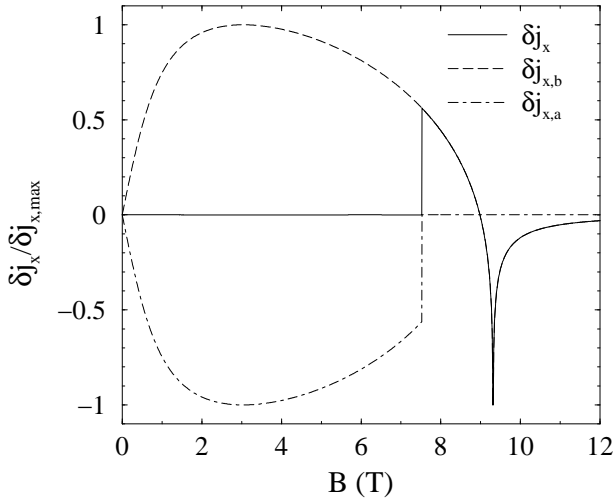


FIG. 2. Calculated magnetic field dependence of the equilibrium diamagnetic current of electrons on the Fermi contour flowing in the right well. Except of the total current also the contributions from the bonding and antibonding subbands are shown: $\delta j_x = \delta j_{x,b} + \delta j_{x,a}$.

As we have mentioned in the introduction, the incomplete balance of chiral diamagnetic currents flowing in the right and left wells is behind the origin of the electron transport in the x direction. In the linear response theory we implicitly assume that applied external

fields are infinitesimally weak. Therefore, also the polarization is weak and only the electrons with energies in a narrow interval around the Fermi energy contribute to the difference between the currents in the left and right wells. For this reason, Fig. 2 presents the calculated equilibrium diamagnetic current $\delta j_{R,x}$ flowing in the right well only for electrons on the Fermi contour. (The current of the opposite direction flows in the left well and $\delta j_{L,x} = -\delta j_{R,x}$.) Together with the total current $\delta j_x (\equiv \delta j_{R,x})$ also the contributions $\delta j_{x,b}$ and $\delta j_{x,a}$ from the bonding and antibonding subbands are shown. In our simplified model $\delta j_{x,b}$ and $\delta j_{x,a}$ exactly cancels out for magnetic fields less than $B_{c,1}$. Above $B_{c,1}$ the current $\delta j_x \equiv \delta j_{x,b}$ decreases and changes sign before the magnetic field reaches $B_{c,2}$. At that field δj_x diverges and for $B > B_{c,2}$ returns slowly back to zero value expected for the decoupled layers. The sharp minima and maxima of the total δj_x reflect qualitative changes of the topology of Fermi contours, caused by the applied in-plane magnetic field, similarly as a field dependence of the DOS.

The results for the conductivity tensor components σ_{xx} and σ_{yy} , calculated assuming zero temperature, are presented in Fig. 3. The overall similarity of curves in Fig. 3 to δj_x is striking. The van Hove singularities at the critical fields $B_{c,1}$ and $B_{c,2}$ seen on δj_x appear also on σ_{xx} and σ_{yy} . Moreover, both components of the conductivity are small below $B_{c,1}$ where δj_x vanishes, are decreasing functions for B between $B_{c,1}$ and $B_{c,2}$, and increase above $B_{c,2}$ similarly as δj_x . But there are, of course, many differences which stem from the more detailed description of the scattering process and response to the external fields, as presented in previous paragraphs.

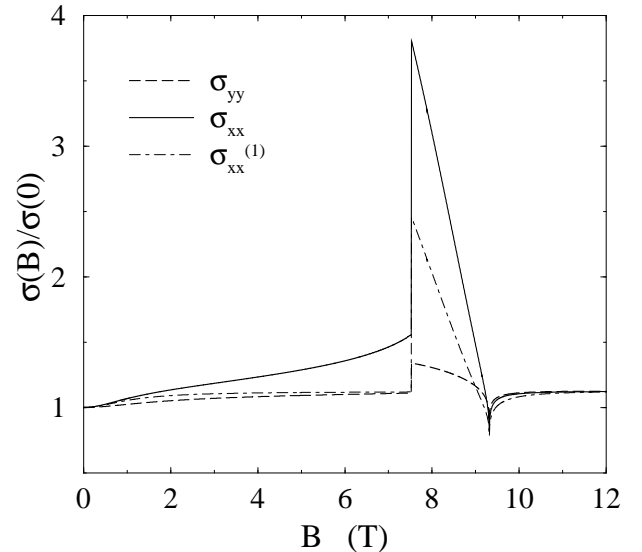


FIG. 3. Magnetic field dependences of the conductivity components σ_{xx} and σ_{yy} . $\sigma_{xx}^{(1)}$ is the conductivity calculated without the Hall correction ($\sigma_{xx}^{(2)}$ neglected).

The dependence of the conductivity components $\sigma_{xx}^{(1)}$

and σ_{yy} on the magnetic field coincides with that already obtained by solving the Boltzmann equation⁵. In this case the origin of the van Hove singularities is related rather to DOS than to δj_x . The difference between $\sigma_{xx}^{(1)}$ and σ_{yy} originates in the Fermi contours anisotropy and the related anisotropy of the effective mass and the relaxation time. The novel “Hall” correction $\sigma_{xx}^{(2)}$ to the conductivity σ_{xx} does not change the field dependence qualitatively, but strengthens the difference between σ_{xx} and σ_{yy} substantially.

The question arises whether one can distinguish between $\sigma_{xx}^{(1)}$ and $\sigma_{xx}^{(2)}$ experimentally. The possibility can be to study the inter-layer charge redistribution by measuring the change of the capacity between the bilayer system and the gate electrode on the top of the sample. It should be proportional to the current flowing through the sample perpendicularly to the magnetic field. The excess electric charge cumulated in the right layer, induced by the applied electric field in the x -direction, is shown in Fig. 4. The maximum effect is expected when only a bonding subband is occupied and the Fermi line has a single-connected-peanut shape.

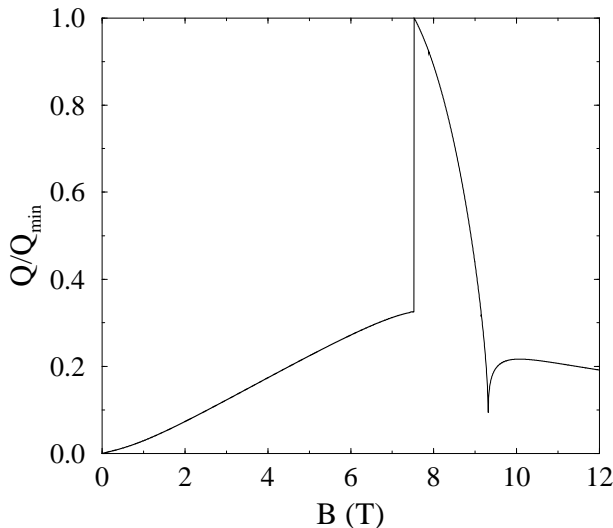


FIG. 4. Charging of the right layer when external electric field is oriented in the x direction. Note that Q is negative.

To conclude: we have shown that the charge redistribution within a double-layer system gives rise to the Hall-like contribution to the conductivity which is so strong that it cannot be omitted. The experimental verification of this Hall effect is however nontrivial. Any potential contacts destroy the double-layer structure heavily and a direct measurement of the potential difference between layers can hardly be realized. We believe that the solution is a non-invasive measurement of the charge redistribution from the capacity changes of gated structures.

ACKNOWLEDGMENTS

This work has been supported by the Grant Agency of the Czech Republic under Grant No. 202/01/0754.

-
- ¹ M. J. Kelly in *Low-dimensional semiconductors* (Oxford University Press, 1995).
 - ² J. A. Simmons, S. K. Lyo, N. E. Harf and J. F. Klem, Phys. Rev. Lett. **73** 2256 (1994)
 - ³ Y. Berk, A. Kamenev, A. Palevski, L. N. Pfeiffer and K. W. West, Phys. Rev. B **51**, 2604 (1995)
 - ⁴ T. Ihn, H. Carmona, P. C. Main, L. Eaves, M. Heinini Phys. Rev. B **50**, 420 (1994)
 - ⁵ O. E. Raichev and F. T. Vasko, Phys. Rev. B **53**, 1522 (1996)
 - ⁶ J. Hu and A. H. MacDonald, Phys. Rev. B **46**, 554 (1992)
 - ⁷ A. Bastin, C. Lewinner, O. Betbeder-Matibet, and P. Nozieres, J. Phys. Chem. Solids **32**, 1811 (1971).
 - ⁸ W. Jones and N. H. March in *Theoretical Solid State Physics* (Wiley, New York, 1973) p. 108